Neisseria gonorrhoeae Penicillin-Binding Protein 3 Exhibits Exceptionally High Carboxypeptidase and β-Lactam Binding Activities[†,‡]

Miglena E. Stefanova,[§] Joshua Tomberg,[||] Melanie Olesky,[||] Joachim-Volker Höltje,[⊥] William G. Gutheil,*[,§] and Robert A. Nicholas*[,||]

Division of Pharmaceutical Sciences, University of Missouri-Kansas City, Kansas City, Missouri 64110, Max-Planck-Institut für Entwicklungsbiologie, D-7400 Tübingen, Germany, and Department of Pharmacology, University of North Carolina at Chapel Hill, Chapel Hill, North Carolina 27599-7365

Received June 19, 2003; Revised Manuscript Received September 29, 2003

ABSTRACT: A soluble form of penicillin-binding protein 3 (PBP 3) from *Neisseria gonorrhoeae* was expressed and purified from *Escherichia coli* and characterized for its interaction with β-lactam antibiotics, its catalytic properties with peptide and peptidoglycan substrates, and its role in cell viability and morphology. PBP 3 had an unusually high k_2/K' value relative to other PBPs for acylation with penicillin (7.7×10^5 M^{-1} s^{-1}) at pH 8.5 at 25 °C and hydrolyzed bound antibiotic very slowly ($k_3 < 4.6 \times 10^{-5}$ s^{-1}, $t_{1/2} > 230$ min). PBP 3 also demonstrated exceptionally high carboxypeptidase activity with a k_{cat} of 580 s^{-1} and a k_{cat}/K_m of 1.8×10^5 M^{-1} s^{-1} with the substrate N^{α}-Boc-N^{ϵ}-Cbz-L-Lys-D-Ala-D-Ala. This is the highest k_{cat} value yet reported for a PBP or other serine peptidases. Activity against a ∼D-Ala-D-Lac peptide substrate was ∼2-fold lower than against the analogous ∼D-Ala-D-Ala peptide substrate, indicating that deacylation is rate determining for both amide and ester hydrolysis. The pH dependence profiles of both carboxypeptidase activity and β-lactam acylation were bell-shaped with maximal activity at pH 8.0−8.5. PBP 3 displayed weak transpeptidase activity in a model transpeptidase reaction but was active as an endopeptidase, cleaving dimeric peptide cross-links. Deletion of PBP 3 alone had little effect on viability, growth rate, and morphology of *N. gonorrhoeae*, although deletion of both PBP 3 and PBP 4, the other low-molecular-mass PBP in *N. gonorrhoeae*, resulted in a decreased growth rate and marked morphological abnormalities.

Penicillin-binding proteins (PBPs)[1] are the lethal targets of penicillin and other β-lactam antibiotics. PBPs synthesize the cell wall peptidoglycan that surrounds the bacteria, and inhibition of these enzymes leads to degradation of the cell wall and eventual cell lysis. All bacteria have multiple PBPs, which act in concert with one another and with other proteins to synthesize nascent peptidoglycan during cell elongation and division (*1*, *2*). These PBPs can be grouped into two classes: the high-molecular-mass (HMM) PBPs, which are essential for cell viability and catalyze transpeptidation and sometimes transglycosylation of disaccharide−pentapeptide chains during peptidoglycan synthesis, and the low-molecular-mass (LMM) PBPs, which are not essential for cell viability and generally catalyze carboxypeptidase and often endopeptidase activity.

Most of our knowledge of the roles of PBPs in cell wall biosynthesis comes from studies in *Escherichia coli*. However, the number of PBPs in this organism complicates these studies. *E. coli* has at least 10 PBPs (PBPs 1A, 1B, 1C, 2, 3, 4, 5, 6, 6b, and 7), although only a few of these proteins appear essential for cell viability (*3*). In contrast to *E. coli*, *Neisseria gonorrhoeae* has only three PBPs, termed PBPs 1, 2, and 3, when [^{3}H]penicillin G-labeled membranes are analyzed by SDS−PAGE and fluorography (*4*). Analysis of the recently completed genomic sequence of *N. gonorrhoeae* (http://www.genome.ou.edu/gono.html) revealed a fourth gonococcal PBP, termed PBP 4 (GenBank accession number AF156692).[2] Of these four PBPs, only PBPs 1 and 2 have been characterized to any extent. PBP 1 is the gonococcal homologue of *E. coli* PBP 1A and likely catalyzes both glycan polymerization and transpeptidation during cell elongation (*5*). PBP 2 is the homologue of *E. coli* PBP 3 and likely functions during cell division (*6*). Alterations in

† Supported by NIH Grants AI-36901 (R.A.N.) and GM-60149 (W.G.G.).

‡ The GenBank accession number for PBP 3 is AF071224.

* To whom correspondence should be addressed: e-mail, nicholas@med.unc.edu (R.A.N.); e-mail, gutheilw@umkc.edu (W.G.G.).

§ University of Missouri−Kansas City.

|| University of North Carolina at Chapel Hill.

⊥ Max-Planck-Institut für Entwicklungsbiologie.

[1] Abbreviations: PBP, penicillin-binding protein; CPase, DD-carboxypeptidase; MBP, maltose-binding protein; TEV, tobacco etch virus; Ac, acetyl; D-Lac, D-lactate; Cbz, benzyloxycarbonyl; Boc, *tert*-butyloxycarbonyl; Ac_2-KAA, Ac-L-Lys(Ac)-D-Ala-D-Ala; BC-KAA, Boc-L-Lys(Cbz)-D-Ala-D-Ala; AcC-KAA, Ac-L-Lys(Cbz)-D-Ala-D-Ala; BAc-KAA, Boc-L-Lys(Ac)-D-Ala-D-Ala; B-KAA, Boc-L-Lys-D-Ala-D-Ala; Ac_2-KA-D-Lac, Ac-L-Lys(Ac)-D-Ala-D-Lac; AMPSO, 3-[(1,1-dimethyl-2-hydroxyethyl)amino]-2-hydroxypropanesulfonic acid; AR, Amplex Red; CAPS, 3-(cyclohexylamino)-1-propanesulfonic acid; OPD, *o*-phenylenediamine; TABS, *N*-[tris(hydroxymethyl)methyl]-4-aminobutanesulfonic acid; TEA, triethylamine; QB, QuantaBlu; SEM, scanning electron microscopy.

[2] P. A. Ropp and R. A. Nicholas, unpublished observations.

10.1021/bi0350607 CCC: $25.00
Published on Web 11/14/2003

both of these PBPs are observed in chromosomally mediated penicillin-resistant strains of *N. gonorrhoeae* (*6*−*8*). These two PBPs are thought to be the only essential PBPs in *N. gonorrhoeae* (*4*), although no studies have addressed this question directly.

The function of *N. gonorrhoeae* PBP 3 in peptidoglycan synthesis is not clear. PBP 3 is readily acylated at low concentrations of penicillin G (*4*), but since cell growth continues at penicillin concentrations that saturate PBP 3, it appears to be nonessential for cell viability. PBP 3 has 29% sequence identity to PBP 4 from *E. coli*, suggesting that this PBP is the gonococcal homologue of *E. coli* PBP 4. *E. coli* PBP 4 is a carboxypeptidase and endopeptidase, but detailed kinetic studies for either of these enzymes have not been reported. Enzymatic characterization of PBPs is required for a better understanding of their physiological role in peptidoglycan biosynthesis and ultimately for the development of new inhibitors for this class of enzymes. Toward this goal we have recently developed high-sensitivity and high-throughput assays for PBP activity against D-Ala substrates (*9*) and D-Lac substrates (*10*) and effective peptide mimetic inhibitors for several LMM PBPs (*11*).

In this study, PBP 3 was overexpressed in *E. coli*, purified to homogeneity, characterized for its β-lactam binding properties and enzymatic activities, and examined for its role in cell growth, viability, and morphology. PBP 3 displayed exceptionally high rates of acylation (k_2/K') with β-lactam antibiotics and of catalytic turnover (k_{cat}) as a DD-carboxypeptidase with peptide substrates. PBP 3 also catalyzed DD-endopeptidase activity, as well as weak transpeptidase activity in the presence of high concentrations of a suitable acyl group acceptor. Deletion of either PBP 3 or PBP 4 was tolerated, but cells with a double deletion in both PBP 3 and PBP 4 grew slower and showed marked morphological abnormalities. The results obtained from this study are relevant to understanding the catalytic and functional properties of this enzyme and of the PBPs in general.

EXPERIMENTAL PROCEDURES

Strains. FA19 is a penicillin-susceptible laboratory strain of *N. gonorrhoeae* (*12*). *E. coli* MC1061 was used for standard subcloning procedures as well as for expression of PBP 3. *N. gonorrhoeae* FA19 was grown on GC medium base agar plates (Difco, Sparks, MD) with supplements I and II (*13*), whereas MC1061 cells harboring the appropriate plasmids were grown in Luria broth supplemented with either 50 mg/mL kanamycin or 100 mg/mL carbenicillin. FA19 was transformed with donor DNA exactly as described previously (*7*). Transformants of strain FA19 by plasmids harboring the PBP 3 and PBP 4 coding sequences disrupted by either the spectinomycin resistance gene [Ω (*14*)] or the kanamycin resistance gene [kpt (*15*)] were selected on GCB agar containing 50 μg/mL spectinomycin and 50 mg/mL kanamycin, respectively.

Cloning of PBP 3 from N. gonorrhoeae. PBP 3 was identified from a Blast search of the *E. coli* genome sequencing project at the University of Oklahoma (B. A. Roe, S. P. Lin, L. Song, X. Yuan, S. Clifton, and D. W. Dyer, www.genome.ou.edu/gono.html) by using the coding sequence of *E. coli* PBP 4 as a query. Up (5′-TTCCCCTGCAAACAAGCCGGTCC-3′) and down (5′-GACCTCTTGCGCCCGATTTACGGA-3′) primers were synthesized according to sequence information in the database, and the coding and flanking sequence of the putative PBP was amplified by PCR from FA19 DNA and subcloned into pBSK-SK+ (pBS-SK+ harboring the kanamycin resistance gene). All of the clones contained inserts in the same orientation, with the 3′ end of the gene closest to the *lac* promoter. Clones from multiple independent amplifications were sequenced on both strands (GenBank accession number AF071224).

Overexpression and Purification of a Soluble Form of PBP 3. The sequence encoding the predicted mature sequence of PBP 3 (PBP 3 lacking its signal sequence amino acids 22−469) and a three amino acid linker (Ala-His-Ala) was fused in-frame to the carboxyl-terminal end of the maltose-binding protein (MBP) in the vector pMAL-C2KV/H_6. pMAL-C2KV/H_6 is similar to pMAL-C2 (New England Biolabs, Beverly, MA) except that it contains the kanamycin resistance gene in place of the β-lactamase gene, a tobacco etch virus (TEV) protease cleavage site at the junction of the two proteins, and six histidine residues between the second and third amino acids of MBP. MC1061 cells harboring the expression plasmid were grown at 37 °C in a 12 L fermentor in enriched broth to an OD_{600} of 1.3, the temperature was lowered to 23 °C, and protein production was induced with 0.3 mM IPTG for 2 h. Cells were harvested, resuspended in 10 mM Tris·HCl, pH 7.5, 2 mM EDTA, and 10% glycerol, and lysed by three passages through a French press (SLM, Rochester, NY) at 16000 psi. Supernatants were obtained by ultracentrifugation at 100000*g*. The fusion protein was precipitated with 55% ammonium sulfate, collected by centrifugation, and redissolved in 50 mM Tris·HCl, pH 8.0, 1 M NaCl, and 10% glycerol (TNG). Following passage through a 0.45 mM filter, the redissolved protein mixture was applied to a Ni^{2+}-chelating column (Amersham Biosciences, Piscataway, NJ), washed with TNG plus 10 mM imidazole, and finally eluted with a 10−300 mM imidazole gradient in TNG. Fractions containing the MBP-PBP 3 fusion protein were pooled, concentrated, and dialyzed against TNG.

The purified fusion protein (7 mL of 8 mg/mL) was cleaved with 0.2 mg of His_6-TEV protease at 30 °C for 3 h. The digests were then reapplied to the Ni^{2+}-chelating column equilibrated in TNG. Analysis of the flow-through fraction revealed several contaminants but no PBP 3. However, PBP 3 was eluted with a TNG/15 mM imidazole wash in a highly purified form. Fractions containing PBP 3 were pooled and dialyzed against 50 mM Tris·HCl, pH 8.0, 500 mM NaCl, and 10% glycerol. The dialyzed protein was then concentrated to ∼2 mg/mL and stored at −80° C.

SDS−PAGE, Binding Stoichiometry, and Gel Filtration. Samples containing PBPs were labeled with [^{125}I]iodopenicillin V (*16*) for 15 min at 30 °C in 10 mM Tris·HCl, pH 8.0, 500 mM NaCl, 1 mM EDTA, and 10% glycerol. The samples were then denatured in SDS−PAGE loading buffer, heated for 3 min at 80 °C, and loaded onto a SDS−10% polyacrylamide gel. Gels were fixed, stained with Coomassie Blue, dried, and visualized by phosphorimaging on a Storm 840 phosphorimager (Molecular Dynamics, Sunnyvale, CA).

To determine the stoichiometry of penicillin G binding, purified PBP 3 (8.9 μg, 180 pmol) was incubated for 15 min at 25 °C with a saturating concentration of [^{14}C]penicillin

G (5 μM), and the covalent [^{14}C]penicillin G−PBP 3 complex was precipitated as described below for determination of k_2/K'. The amount of labeled complex was quantitated by converting disintegrations per minute (dpm) to moles of [^{14}C]penicillin G bound (specific activity = 1.1×10^8 dpm/μmol).

For gel filtration, PBP 3 (250 μg, 5.1 nmol) was incubated with 5 μM [^{14}C]penicillin G in a 130 μL total volume. After 15 min at 25 °C, the mixture was diluted to 400 μL with 10 mM Tris·HCl, pH 8.0, and carried through two cycles of concentration/dilution in a Microcentricon 30 (Amicon Corp., Boston, MA) in order to lower the free [^{14}C]penicillin G concentration. The sample was then loaded onto a 16 × 600 mm Sephacryl S-200HR column (Amersham, Piscataway, NJ) equilibrated in 20 mM Tris·HCl, pH 8, and 150 mM NaCl, and the [^{14}C]penicillin G−PBP 3 complex was eluted in the same buffer. Fractions of 2 mL were collected, and 250 μL aliquots were submitted to scintillation counting to determine the elution position of the labeled complex. A separate chromatographic run established the elution positions of several protein standards.

Determination of Acylation and Deacylation Rate Constants for β-Lactam Antibiotics. The kinetic scheme for the interaction of a PBP with either substrate or a β-lactam antibiotic is

$$E + S \underset{k_{-1}}{\overset{k_1}{\rightleftarrows}} E{\cdot}S \xrightarrow{k_2} E{-}S \xrightarrow{k_3} E + P \qquad (1)$$

where E·S is the noncovalent Michaelis complex, E−S is the covalent acyl-enzyme complex, and P is the released product. The constant k_2/K', in which $K' = (k_{-1} + k_2)/k_1$, describes the initial rate of formation of covalent β-lactam antibiotics−target conjugates (E−S) at low (subsaturating) concentrations of β-lactam antibiotics (*17*). k_2/K' constants were determined from time courses of formation of acyl-enzyme complexes. Preliminary experiments revealed that PBP 3 had a very high rate of acylation with [^{14}C]penicillin G. Thus, to ensure that [^{14}C]penicillin G was present in at least a 10-fold molar excess over PBP 3 and that the experimental rate of acylation was slow enough to measure, it was necessary to measure k_2/K' at a single low concentration (0.25 μM) of [^{14}C]penicillin G at 25 °C. PBP 3 (8.9 mg, 180 pmol) was diluted into 7.3 mL of 0.25 μM [^{14}C]-penicillin G in 50 mM sodium phosphate, pH 7.0, and 10% glycerol to a final concentration of 24 nM. At 15 s intervals, 920 μL aliquots were removed, mixed with 5 mL of 5% trichloroacetic acid (w/v), and incubated on ice for 15 min. The acidified proteins were passed through no. 30 glass fiber filters (Schleicher and Schuell, Keene, NH), and the filters were washed twice with 5 mL each of 1% trichloroacetic acid and 33% methanol. The filters were then air-dried, placed in scintillation vials with 3 mL of Scinti-safe scintillation fluid (Fisher Scientific, Pittsburgh, PA), and counted. Sodium pyrophosphate (pH 5.5−9) or carbonate (pH 9.5−10.5) buffers were used to determine the pH dependence of k_2/K'.

k_2/K' constants for imipenem, ampicillin, and ceftriaxone were determined by the competition method against [^{14}C]-penicillin G (*17*). A fixed concentration of [^{14}C]penicillin G (0.5 μM) and concentrations of the unlabeled antibiotics that inhibited binding by approximately 50% were incubated with PBP 3 in sodium phosphate buffer, pH 7, at 25 °C for 3 min, and the level of radioactivity bound to the proteins was quantitated as described above. Equation 2 was used to

$$(k_2/K')_U = (k_2/K')_L \frac{(EC_0 - EC_U)C_L}{(EC_U)C_U} \qquad (2)$$

calculate k_2/K' constants, where EC_0 and EC_U represent the amount of acyl-enzyme complex formed in the absence and presence of unlabeled antibiotic, respectively, and C_U and C_L are the concentrations of unlabeled and labeled antibiotic, respectively.

The deacylation rate constant was derived from the first-order decay rates of the [^{14}C]penicilloyl−PBP 3 complex. PBP 3 (18 μg, 7.4 μM) was incubated for 5 min with 145 μM [^{14}C]penicillin in 50 mM sodium phosphate, pH 7, and 10% glycerol. The mixture (50 μL) was then diluted into 7 mL of 50 mM sodium phosphate, pH 7, 10% glycerol, and 11.4 mM penicillin G, and 1 mL aliquots were removed at various times and diluted into 4 mL of 5% TCA on ice. The amount of [^{14}C]penicillin remaining bound to PBP 3 was determined following filtration through glass fiber filters and scintillation counting as described above. The k_3 constant was determined by dividing 0.693 by the half-life in seconds (derived from plots of log percent bound versus time).

Carboxypeptidase Assays. Carboxypeptidase (CPase) activity against ~D-Ala-D-Ala-based substrates was determined by the fluorescence assay methods for D-Ala detection described previously (*9*). The synthetic PBP substrate Ac-L-Lys(Ac)-D-Ala-D-Ala (Ac_2-KAA) was used at a concentration of 2 mM unless otherwise noted. Control experiments confirmed that enzymatic activity was linear for up to 1.5 h. To determine the substrate specificity of PBP 3, peptide substrates with different substituents on the N^{α}- and N^{ϵ}-amino groups of lysine in L-Lys-D-Ala-D-Ala were used at concentrations ranging from 0 to 50 mM. Activity against the depsipeptide substrate Ac_2-KA-D-Lac was determined by detection of D-Lac using D-lactate dehydrogenase as described previously (*10*) but with NADH levels measured by fluorescence (ex_{325nm}, em_{465nm}). D-Lac was used as a standard. All enzyme assays were performed at 25 °C in microtiter plates, and absorbance or fluorescence was read in a Tecan SpectraFluor Plus microtiter plate reader (Research Triangle Park, NC).

Data Analysis. Data were analyzed by fitting with the appropriate equation by nonlinear regression using BMDP statistical software (SPSS Science, Chicago, IL). The form of the Michaelis−Menten equation shown in eq 3 was used to obtain the value and standard error (SE) for k_{cat} and K_m, and the form of this equation shown in eq 4 was used for the value and SE for k_{cat}/K_m. In the case of BC-KAA and

$$\frac{v}{E_T} = \frac{k_{cat}[S]}{K_m + [S]} \qquad (3)$$

$$\frac{v}{E_T} = \frac{(k_{cat}/K_m)K_m[S]}{K_m + [S]} \qquad (4)$$

AcC-KAA, significant substrate inhibition was observed (Figure 2). In these two cases, only the data points from 0 to peak activity were included in the statistical analysis. In

all cases the k_{cat}/K_m values, which reflect the activity of the enzyme at subsaturating substrate concentration, will be accurate. However, for substrates that exhibit substrate inhibition, the apparent K_m will be lower than the true K_m, as will k_{cat}. Since the possibility of less apparent substrate inhibition also exists for the other substrates, the values for k_{cat} and K_m reported in Table 2 are given as the apparent values and are the minimum values for these parameters.

Transpeptidase Assays. Transpeptidase reactions were performed with Ac_2-KAA (10 mM) as the acyl group donor and variable concentrations of glycine as the acyl group acceptor (*18*, *19*). PBP 3 was used at a concentration sufficient to convert 5−10% of substrate to products, which was adequate for accurate product determination by HPLC. The relatively large amount of D-Ala hydrolysis product was determined in *o*-phenylenediamine-based microtiter plate assays as described previously (*10*, *20*). The accumulation of transpeptidase (Ac_2-KAG) and hydrolase (Ac_2-KA) products was followed by reverse-phase HPLC on a C_{18} column (5 μm, 0.46 × 25 cm) with a water/acetonitrile gradient. The column was equilibrated in 100% A, and samples were eluted with a gradient of 0−25% B in 15 min [A = 0.1% (v/v) trifluoroacetic acid in water; B = 0.1% (v/v) trifluoroacetic acid in 70% acetonitrile/30% water].

pH Dependence and pH Stability. The effect of pH on CPase activity was studied, using a range of overlapping buffers, in 50 mM buffer, 100 mM NaCl, and 0.5 mg/mL alkylated BSA, pH 3.5−12.25. For pH stability studies the enzyme was preincubated in 20 mM buffer for 60 min at 25 °C, then the pH was shifted to 8.5 with 100 mM pyrophosphate, 100 mM NaCl, and 0.5 mg/mL alkylated BSA, and the standard enzyme assay was performed. The lower buffer concentration used in the pH stability studies allowed for the pH shift to be completed with the standard activity assay buffer concentration. At subsaturating substrate concentrations the following model applies:

$$EH_2 \overset{pK_1\ (acidic)}{\longleftrightarrow} EH + H^+ \overset{pK_2\ (basic)}{\longleftrightarrow} E + H^+ \quad (5)$$

$$EH + S \overset{(k_{cat}/K_m)_{EH}}{\longrightarrow} EH + P \quad (6)$$

The following equation was used to fit the data:

$$\frac{v}{E_T} = \frac{[S]\cdot[H^+]\cdot(k_{cat}/K_m)_{EH}}{K_2(1 + [H^+]/K_2 + [H^+]^2/(K_1K_2))} \quad (7)$$

where $(k_{cat}/K_m)_{EH}$ represents the activity of the monoprotonated enzyme, $[H^+] = 10^{-pH}$, $K_1 = 10^{-pK_1}$, and $K_2 = 10^{-pK_2}$. Values for $(k_{cat}/K_m)_{EH}$, pK_1, and pK_2 were obtained by fitting the data to eq 7 by nonlinear regression with BMDP statistical software. The same equations were used to estimate pK_1 and pK_2 for the pH dependence of [^{14}C]penicillin G binding.

Endopeptidase Activity. Endopeptidase activity was determined by incubating purified high-molecular-mass murein sacculi (*21*) with purified PBP 3 followed by analysis of the changes in murein structure as compared to an untreated control. Accordingly, the murein samples were digested completely with Cellosyl (kindly provided by Dr. Aretz, Aventis, Germany). The resulting muropeptides were reduced with sodium borohydride and separated by reverse-phase HPLC on a 3 mm ODS column as previously described (*22*).

Scanning Electron Microscopy. Cultures (50 mL) of FA19, FA19 PBP3::Ω, FA19 PBP4::*kpt*, and FA19 PBP3::Ω PBP4::*kpt* were grown at 37 °C in GCB broth with supplements A, I, and II and 10 mM sodium bicarbonate (*13*) to an OD_{600} of 0.7 and then pelleted at 2000*g*. The cells were washed twice with phosphate-buffered saline containing 10 mM $MgCl_2$ and then resuspended in 1 mL of the same buffer. Ten milliliters of 2.5% glutaraldehyde in phosphate-buffered saline was added, and the cells were rocked for 10 min. The cells were then filtered through a 0.1 μm Nucleopore polycarbonate filter (Whatman), dehydrated through a series of increasing ethanol concentrations, critical-point dried, encoded with gold palladium, and submitted to scanning electron microscopy on a Cambridge Instruments Stereoscan S-200 instrument (LEO Electron Microscopy Ltd., Thornwood, NY) at the Microscopy Core Facility at the University of North Carolina at Chapel Hill.

RESULTS

Cloning and Expression of PBP 3 from N. gonorrhoeae. The *dacB* gene encoding PBP 3 from *N. gonorrhoeae* was amplified from the genome of the penicillin-susceptible strain FA19 and cloned into pBSK-SK. All of the clones obtained contained the PBP 3 gene in the opposite orientation of the *lac* promoter. Moreover, our initial attempts to clone full-length PBP 3 containing its signal sequence into several *E. coli* expression vectors (pT7-7, pET-15b, pTTQ18) were unsuccessful, as all of the plasmid constructs contained frame-shift mutations. These results suggest that even low (i.e., noninduced) levels of gonococcal PBP 3 expressed in the periplasm of *E. coli* are lethal. To avoid problems associated with periplasmic expression, we expressed the mature protein (lacking the signal sequence) in the cytoplasm as a fusion protein with maltose-binding protein (MBP).

The cleavage site of the signal sequence of PBP 3 predicted with either SignalP (*23*) or PSORT (*24*) programs is between Ala-21↓Leu-22. Thus, the coding sequence from Leu-22 to the C terminus (and a short linker sequence, Ala-His-Ala) was fused in-frame to the carboxyl terminus of His_6-tagged MBP, and the fusion protein was expressed in *E. coli*. Soluble expression of the fusion protein in the cytoplasm was possible since PBP 3, unlike most other PBPs, does not contain a hydrophobic anchor that promotes association with the membrane bilayer (*25*). PBP 3 was purified as described in Experimental Procedures, and the final preparation had a concentration of 2 mg/mL and was greater than 95% pure (Figure 1A).

Characterization of Purified PBP 3. Because PBPs form a covalent complex with β-lactam antibiotics, PBPs incubated with a radioactive β-lactam can be visualized following SDS−PAGE and autoradiography (*26*). The purified protein was incubated with 5 mg/mL [^{125}I]iodopenicillin V for 10 min at 30 °C, followed by SDS−PAGE and phosphorimaging (Figure 1B). PBP 3 represented the major radiolabeled band, although two minor bands were also present. The slower migrating band runs at a position expected of a dimer of PBP 3, while the faster migrating band is likely a proteolytic breakdown product. Furthermore, recombinant PBP 3 comigrated with PBP 3 from membranes prepared

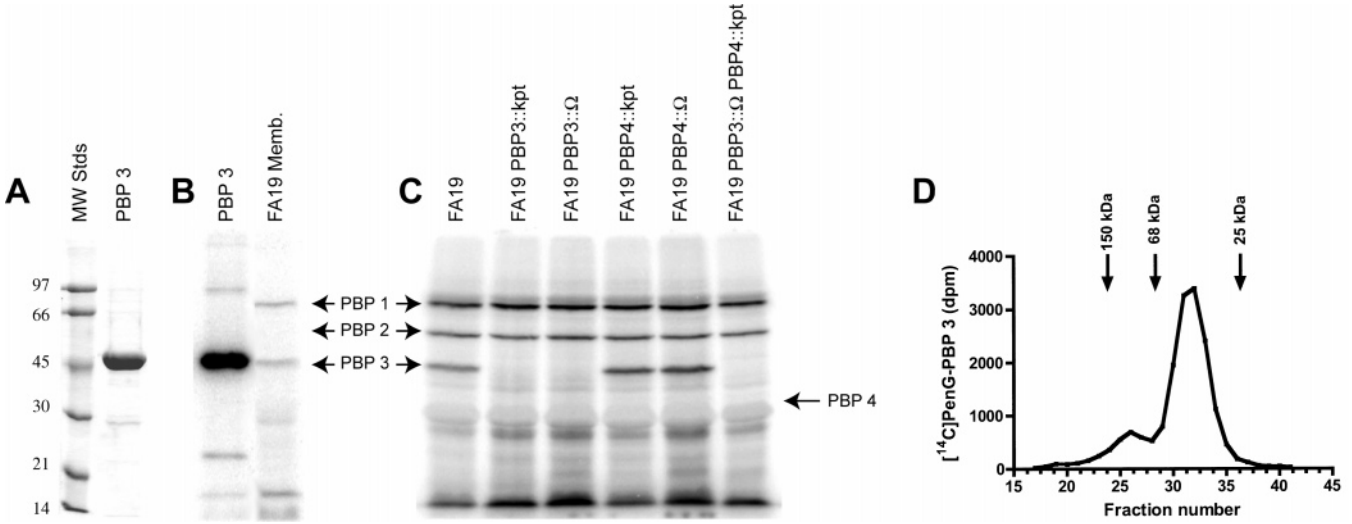

FIGURE 1: SDS−PAGE of cell lysates and membranes from *N. gonorrhoeae* containing deletions in the genes encoding PBP 3 and/or PBP 4. (A) Coomassie-stained 10% polyacrylamide−SDS gel of protein standards (molecular masses in kDa) and 3 μg of purified PBP 3. (B) Phosphorimage of [^{125}I]iodopenicillin V-labeled PBP 3 (3 μg) and FA19 membranes (20 μg). (C) Phosphorimage of [^{125}I]iodopenicillin V-labeled cell lysates from the indicated gonococcal strains. The positions of PBPs 1−4 are indicated by the arrows. (D) Gel filtration of [^{14}C]penicillin G-labeled PBP 3. The elution positions of protein standards are shown at the top of the elution profile.

Table 1: k_2/K' Values for Interaction of PBP 3 with β-Lactam Antibiotics[a]

β-lactam antibiotic	k_2/K' (M^{-1} s^{-1})
[^{14}C]penicillin G	200000 ± 30000
imipenem	270000 ± 40000
ceftriaxone	64000 ± 7000
ampicillin	37000 ± 4000

[a] k_2/K' values were derived from a time course of acylation by [^{14}C]penicillin G or by the competition method (*17*) in sodium phosphate buffer, pH 7.0. The values represent the average ± SD for four separate determinations.

Table 2: Apparent Kinetic Parameters for Hydrolysis of D-Ala- and D-Lac-Based Substrates

substrate	k_{cat}/K_m (M^{-1} s^{-1})	K_m[a] (mM)	k_{cat}[a] (s^{-1})
BocCbz-KAA	180000 ± 30000	3.3 ± 0.8	580 ± 60
BocAc-KAA	62000 ± 6000	6.5 ± 0.8	400 ± 10
AcCbz-KAA	142000 ± 6000	3.7 ± 0.2	530 ± 10
Ac_2-KAA	29000 ± 2000	19 ± 2	550 ± 20
BocH-KAA	8300 ± 400	32 ± 3	260 ± 10
Ac_2-KA-D-Lac	12300 ± 800	28 ± 3	340 ± 20

[a] Minimum apparent value, as discussed in the text.

from *N. gonorrhoeae* strain FA19 (Figure 1B). Saturation binding studies of PBP 3 and [^{14}C]penicillin G indicated that PBP 3 bound [^{14}C]penicillin G with a stoichiometry of 1.02 ± 0.07 mol/mol ($n = 29$), indicating that the protein retained complete activity following purification. Taken together, these data indicate that the cloned gene encodes PBP 3.

Several studies have demonstrated that at least some PBPs, e.g., *E. coli* PBP 1B, exist under normal conditions as a dimer (*27*, *28*). To determine the oligomeric state of PBP 3, the [^{14}C]penicillin G−PBP 3 complex was submitted to gel filtration on a Sephacryl S-200 column (Figure 1D). The majority of the radioactivity eluted at a position consistent with a PBP 3 monomer, with a small amount of radioactivity eluting in earlier fractions. The mass of this smaller peak is consistent with the slower migrating band observed on SDS−PAGE (Figure 1B).

Interaction of PBP 3 with β-Lactam Antibiotics. The interaction of β-lactam antibiotics with a PBP is described by the k_2/K' acylation rate constant, which is derived from time courses of acyl-enzyme complex formation (*17*). PBP 3 had a very high k_2/K' acylation rate with [^{14}C]penicillin G (2.0×10^5 M^{-1} s^{-1}) in phosphate buffer and 10% glycerol, pH 7.0, at 25 °C (Table 1). The k_2/K' values for the nonradioactive antibiotics, imipenem, ampicillin, and ceftriaxone, were determined by the competition method (*17*) and ranged from 2.7×10^5 M^{-1} s^{-1} for imipenem to 3.7×10^4 M^{-1} s^{-1} for ampicillin (Table 1). The k_3 rate constant for deacylation of bound [^{14}C]penicillin G was slow, with a half-life of the acyl-enzyme complex of 250 min ($k_3 = 4.6 \times 10^{-5}$ s^{-1}).

Carboxypeptidase and Transpeptidase Activities of PBP 3. PBP 3 was also exceptionally active as a carboxypeptidase (CPase). The enzyme had the highest activity against BC-KAA, with a k_{cat}/K_m of 1.8×10^5 M^{-1} s^{-1} and a k_{cat} of 580 s^{-1} (Table 2). Significant variation in the substrate saturation profiles with various peptides was observed (Figure 2). Two substrates, BC-KAA and AcC-KAA, demonstrated substantial substrate inhibition. The other four substrates all demonstrated some degree of saturation without apparent substrate inhibition. Notably, the D-Lac-based substrate, Ac_2-KA-D-Lac, was a poorer substrate than the corresponding D-Ala-based substrate, Ac_2-KAA. For comparison, the prototypical D-alanine CPase PBP 5 from *E. coli* hydrolyzes Ac_2-KAA and Ac_2-KA-D-Lac with k_{cat}/K_m values of 10 and 700 M^{-1} s^{-1}, respectively (*10*, *29*) (Table 5). Thus, PBP 3 is nearly 3000-fold more active than *E. coli* PBP 5 on Ac_2-KAA but does not show an increase in k_{cat} with D-Lac-containing depsipeptide substrates.

In the presence of a suitable acceptor, many CPases catalyze a model transpeptidase reaction (*18*). PBP 3 demonstrated weak transpeptidase activity with Ac_2-KAA as an acyl group donor and glycine as an acyl group acceptor (Figure 3). The glycine concentration at which the amount of hydrolysis product was equal to that of transpeptidation product could not be reached (>100 mM). High concentrations of glycine were observed to inhibit the total enzyme turnover (D-Ala production) by about 25%.

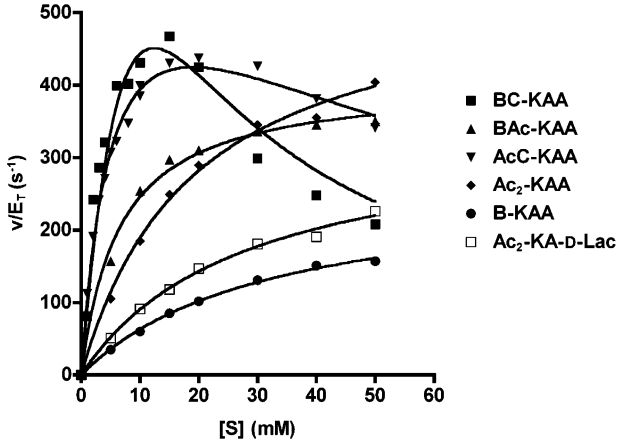

FIGURE 2: Substrate specificity of PBP 3 toward various substrates. CPase activity was assayed under standard conditions. The enzyme concentration was 0.07 nM except in the Ac_2-KA-D-Lac experiment (2 nM). All of the reactions ran for 45 min. Note the substantial substrate inhibition at higher concentrations of BC-KAA and AcC-KAA (see text for explanation).

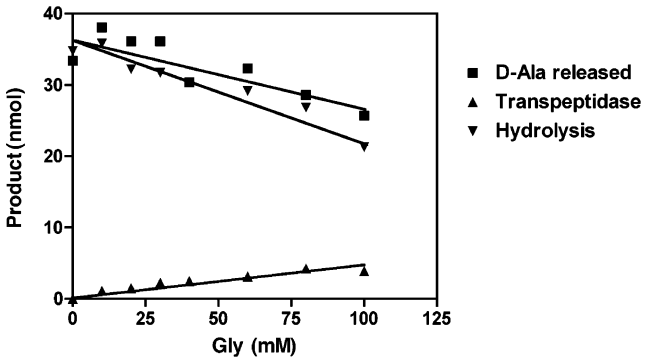

FIGURE 3: Effect of glycine concentration on transpeptidase activity catalyzed by PBP 3. The reaction mixture contained 1.1 nM PBP 3 and 10 mM Ac_2-KAA in standard assay buffer. Glycine concentrations varied from 0 to 100 mM. Samples were incubated for 75 min, the reaction was stopped by the addition of 50 mg/mL ampicillin, and the resulting mixtures were analyzed for the various end products as described in Experimental Procedures.

A broad range of general enzyme inhibitors and reagents, previously assessed as *E. coli* PBP 5 inhibitors (*29*) and including serine protease inhibitors, cysteine-alkylating reagents, metal chelators, and alkali metal salts, were tested for their ability to inhibit the CPase activity of PBP 3 with Ac_2-KAA as a substrate (data not shown). Very few of these reagents, when present at 1 mM, were capable of inhibiting PBP 3. Of the reagents tested, only phenylboronic acid (76% inhibition) and *N*-chlorosuccinimide (95% inhibition) significantly inhibited the hydrolytic activity of PBP 3.

pH−Activity Profiles of CPase Activity and β-Lactam Binding. The pH dependence of k_{cat}/K_m for CPase activity with Ac_2-KAA is shown in Figure 4A. PBP 3 had a bell-shaped pH profile with an optimum in the range 7.5−9.5. There was a gap in the activity at pH 9 when a shift from pyrophosphate to more alkaline buffers was made. pK_as were 6.8 ± 0.1 and 9.8 ± 0.2 for the ascending and descending limbs of the pH versus activity profile. The alkaline gap somewhat complicated this analysis. Closing the alkaline gap by adjusting the alkaline pH data had a significant effect on the fit value for the alkaline pK_a (0.5 pH unit increase), whereas the acidic pK_a was unaffected. Data for triethylamine

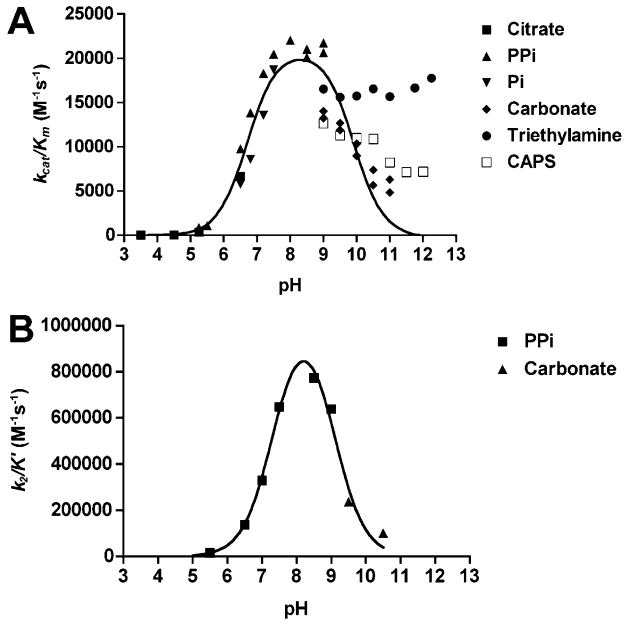

FIGURE 4: pH profiles of PBP 3 for CPase activity and antibiotic binding. (A) pH profile of k_{cat}/K_m for PBP 3-catalyzed hydrolysis of Ac_2-KAA. The enzyme concentration was 1.4 nM, and the reaction time was 30 min. D-Ala was detected with QB assays. The solid line represents the best-fit curve based on fit parameter values of pK_1 = 6.8 (0.1) and pK_2 = 9.8 (0.2). (B) pH dependence of the k_2/K' constant for acylation of PBP 3 by [^{14}C]penicillin G. The solid line represents the best-fit curve based on fit parameter values of pK_1 = 7.3 (0.1) and pK_2 = 9.1 (0.1). Experimental conditions are described in Experimental Procedures.

(TEA) and 3-(cyclohexylamino)-1-propanesulfonic acid (CAPS) demonstrated anomalous behavior and were excluded from statistical analysis of the data. None of the buffers had an adverse effect on enzyme stability (data not shown).

The pH dependence of *β*-lactam acylation was very similar to that for CPase activity. The k_2/K' values became measurable at pH values >5.5, reached an apparent maximum of ~8 × 10^5 M^{-1} s^{-1} at pH 8.5, and declined at higher pH (Figure 4B). The k_2/K' value at pH 8.5 is the highest ever reported by a PBP for penicillin G. The pK_as derived from the ascending and descending limbs of the pH profile of penicillin acylation were 7.3 ± 0.1 and 9.1 ± 0.1, respectively. These values were similar to the pK_as derived for CPase activity without adjusting the alkaline gap. There was a discrepancy in the k_2/K' values derived from these experiments (obtained in sodium pyrophosphate buffers) compared to the value obtained in sodium phosphate buffer at pH 7.0, suggesting that the composition of the buffer influences penicillin binding. This was confirmed by determining k_2/K' in both phosphate and pyrophosphate buffers at pH 7.0, which indicated that pyrophosphate stimulated penicillin binding 1.7-fold compared to phosphate buffer (3.3 × 10^5 versus 2.0 × 10^5 M^{-1} s^{-1}, respectively).

Endopeptidase Activity of PBP 3. PBP 4 from *E. coli*, the apparent homologue of PBP 3 from *N. gonorrhoeae*, has been reported to catalyze endopeptidase activity (*30*). Thus, we also tested PBP 3 for its ability to hydrolyze peptide cross-links in isolated murein and in purified bis(disaccharide)-pentapeptide dimers. PBP 3 cleaved both isolated murein and purified bis(disaccharide)-pentapeptide dimers,

Table 3: Endopeptidase Activity of PBP 3 on High-Molecular-Mass Murein Sacculi[a]

	control	PBP 3 treated
total dimers	41.4/43.3	8.6/8.6
DD cross-links	36.0/35.7	2.2/0.9
LD cross-links	4.9/7.2	6.0/7.1
total trimers	6.0/4.5	2.5/0.9
DD trimers	5.4/4.0	2.5/0.8
LD trimers	0.8/0.2	0.6/0.1

[a] Isolated murein sacculi were incubated with buffer or PBP 3, digested to completion with Cellosyl, and reduced with sodium borohydride (*21*). The resulting samples were then separated on HPLC (*22*). Values shown are the percentage of the total area of HPLC peaks. Data are from two independent experiments.

indicating that PBP 3, like *E. coli* PBP 4, is active as an endopeptidase (Table 3). PBP 3 appeared to be strictly a DD-endopeptidase with little to no LD-endopeptidase activity.

Role of PBP 3 in Cell Viability, Growth, and Morphology. To investigate the role of PBP 3 in the growth and viability of *N. gonorrhoeae*, the chromosomal gene encoding PBP 3 was deleted from the laboratory strain FA19 via homologous recombination. The PBP 3 gene cloned in pBluescript was interrupted by either the kanamycin phosphotransferase (*kpt*) or spectinomycin resistance gene (Ω), and these constructs were used to transform competent FA19 cells to kanamycin or spectinomycin resistance, respectively. Resistant colonies were isolated at a frequency of $\sim 1 \times 10^{-4}$, suggesting that the PBP 3 gene is not essential for cell viability. To confirm that the gene product was no longer expressed in these cells, membranes were prepared from FA19, FA19 PBP3::*kpt*, and FA19 PBP3::Ω, incubated with [^{125}I]IPV for 10 min at 30 °C, and submitted to SDS−PAGE and phosphorimaging. As seen in Figure 1C, cell lysates from both PBP 3 deletion strains showed no detectable [^{125}I]IPV binding at the position of PBP 3.

N. gonorrhoeae contains one additional LMM PBP, PBP 4 (Stefanova et al., in press). Previous studies have demonstrated that certain bacteria, such as *E. coli*, can survive in the absence of multiple LMM PBPs (*3*), but the roles of LMM PBPs in the growth of *N. gonorrhoeae* have not been investigated. Thus, the viability of FA19 missing both PBP 3 and PBP 4 was also determined. The coding sequence of PBP 4 was disrupted by insertion of the kpt resistance gene and transformed into FA19 PBP3::Ω. Strains of FA19 containing deletion of PBP 4 alone were also generated. Transformants were selected for kanamycin resistance at a frequency of $\sim 4 \times 10^{-5}$, suggesting that both PBP 3 and PBP 4 are dispensable for cell viability in the gonococcus. Surprisingly, no [^{125}I]IPV-labeled band migrating at the position of PBP 4 could be detected in either cell lysates (Figure 1C) or membranes (data not shown) from any of the strains examined. Thus, PBP 4 is either expressed at very low levels or is repressed under laboratory growth conditions.

To examine the effect of PBP deletions on cell growth rates, doubling times of cultures of FA19, FA19 PBP3::Ω, FA19 PBP4::*kpt*, and FA19 PBP3::Ω PBP4::*kpt* were determined (Table 4). These data indicated that whereas the doubling times of the single PBP deletion strains were not significantly different from that of FA19, the double deletion strain grew significantly slower ($P < 0.05$). Thus, although bacteria were viable in the absence of all LMM PBPs, they did not grow as rapidly as the wild type or single deletion strains.

Table 4: Growth Rates of *N. gonorrhoeae* Containing Deletions in PBP 3 and/or PBP 4[a]

strain	av doubling times ($n = 4$)
FA19	1.5 ± 0.2
FA19 PBP3::Ω	1.6[b]
FA19 PBP4::*kpt*	1.7 ± 0.1
FA19 PBP3::Ω PBP4::*kpt*	1.9[c] ± 0.2

[a] The doubling times were obtained as described in Experimental Procedures and averaged over four separate experiments. [b] All four experiments gave the same doubling time. [c] Significantly different from FA19 ($P < 0.05$).

To determine the effects of these mutations on cell morphology, cells from each of the four strains were prepared as described in Experimental Procedures and submitted to scanning electron microscopy (SEM). As shown in Figure 5, FA19 cells displayed the normal diplococcus morphology, and all of the cells were of similar size. FA19 cells in which either PBP 3 or PBP 4 was inactivated individually were very similar to wild-type cells. In contrast, marked morphological abnormalities were observed in FA19 lacking both PBPs. There was considerable variation in cell size, with some very large cells and cells that were considerably smaller than wild-type cells, suggesting an aberrant initiation site of the division septa. Taken together with our growth rate results, these data demonstrate that deletion of PBPs 3 and 4 together affect cell growth and morphology and further suggest that PBP 4, even though it is not visible on autoradiographs following SDS−PAGE, has a physiological role in cell wall synthesis in *N. gonorrhoeae*.

DISCUSSION

Our initial interest in *N. gonorrhoeae* arose from its ability to become resistant to antibiotics through alterations of endogenous genes, each of which incrementally increases the minimum inhibitory concentration of the antibiotic until treatment failure occurs. However, *N. gonorrhoeae* also is a useful model organism in which to study PBP structure and function. These bacteria have a relatively simple cohort of four PBPs (PBPs 1−4) compared to the ten PBPs expressed in *E. coli*. In particular, PBP 3 is the most highly expressed PBP in gonococcal membranes, but very little is known about its role in cell wall biosynthesis or its catalytic activity. In this study, *N. gonorrhoeae* PBP 3 was expressed and purified from *E. coli* and characterized for its enzymatic activity, β-lactam binding properties, and its physiological role in cell wall synthesis. Our results indicate that although PBP 3 is not essential for cell viability, it displays exceptionally high CPase and β-lactam antibiotic binding activities, with some of the highest values reported to date for PBPs.

Initial efforts to express PBP 3 in the periplasm of *E. coli* with its cleavable signal sequence intact were unsuccessful. This result is likely due to the high enzymatic activity of PBP 3, which would disrupt cross-linking of the peptide chains and destabilize the cell wall. To circumvent this obstacle, PBP 3 lacking its signal sequence was expressed as a MBP fusion protein in the cytoplasm of *E. coli*, which allowed for the purification of large amounts of functionally active protein. Interestingly, overexpression of PBP 3 missing

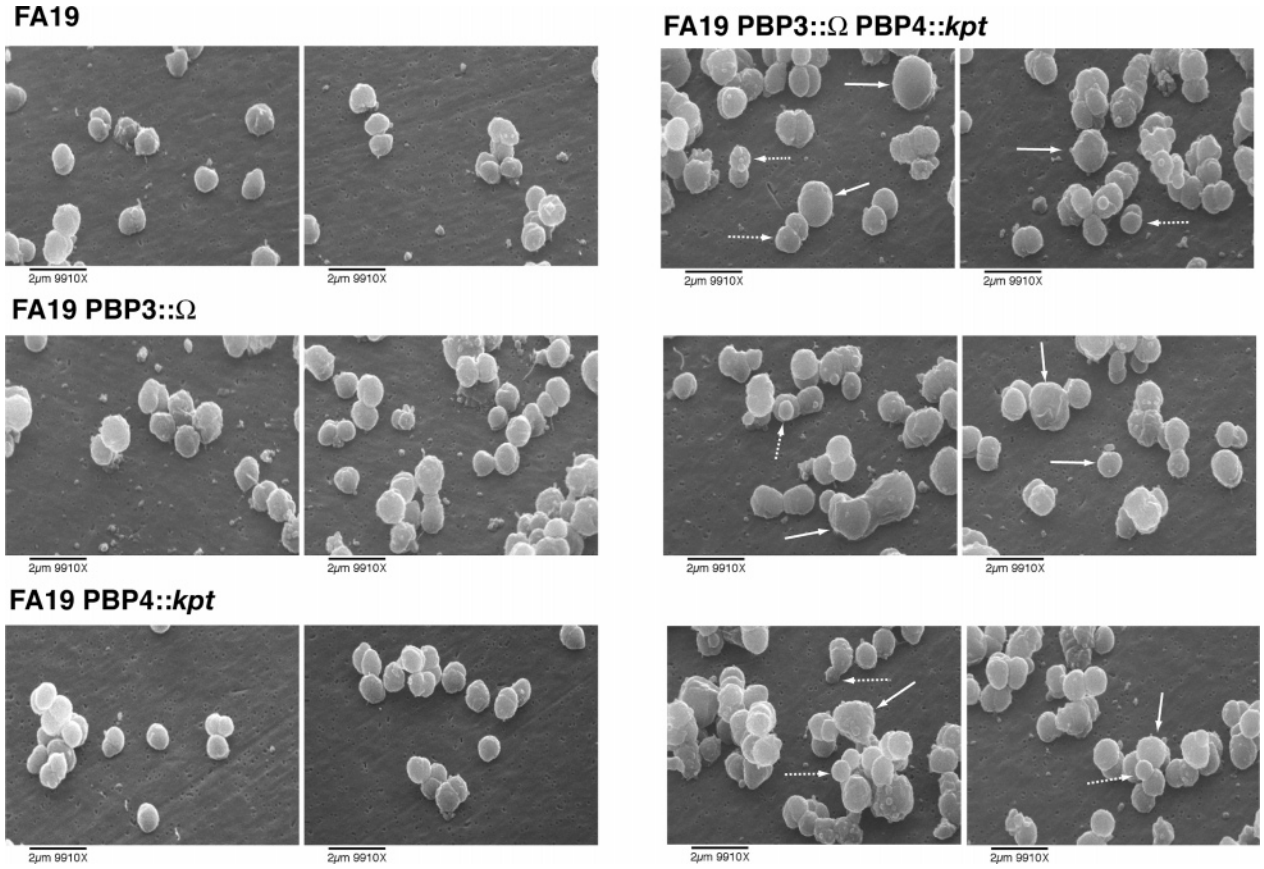

FIGURE 5: Scanning electron micrographs of *N. gonorrhoeae* strains. FA19, FA19 PBP3::Ω, FA19 PBP4::*kpt*, and FA19 PBP3::Ω PBP4::*kpt* cultures were prepared as described in Experimental Procedures and submitted to SEM. The arrows on the right panels identify either very large cells (solid arrow) or very small cells (dashed arrow) relative to wild type or the single deletion strains.

only its signal sequence resulted in a soluble protein, even though native PBP 3 in *N. gonorrhoeae* is found exclusively in the membrane fraction of a cell lysate. The solubility of PBP 3 is in contrast to most other PBPs (such as gonococcal PBP 2 and *E. coli* PBP 5), which contain hydrophobic membrane anchors that mediate interaction of the PBP with the lipid bilayer (*31*, *32*). Since we did not remove any sequence that might act as a membrane anchor, PBP 3 must associate with the membrane in an indirect manner by an unknown mechanism. The solubility of its closest homologue, *E. coli* PBP 4 (*25*), as well as another PBP, the K15 DD-peptidase from *Streptomyces* K15 (*33*), has also been noted. There are no obvious hydrophobic regions in hydropathy plots of the primary sequences of either PBP 3 or the other two PBPs mentioned above. However, the structure of the K15 DD-peptidase revealed the presence of a four-stranded β-sheet domain not found in other LMM PBP structures, which was hypothesized to mediate its interaction with the cell membrane and/or peptidoglycan (*34*).

PBP 3 displayed a very high rate of acylation by β-lactam antibiotics, with the k_2/K' value for [^{14}C]penicillin G of 7.7 $\times$ 10^5 M^{-1} s^{-1} at pH 8.5 being the highest value yet reported. The k_2/K' of imipenem was even higher than that for penicillin G. It should be noted that because of the high rate of acylation these values were obtained at 25 °C. Thus, the values at 30 or 37 °C (the temperature at which most other PBPs are assayed) are likely to be even higher. By comparison, the k_2/K' constants range from 100 to ~3000 M^{-1} s^{-1} for acylation of *E. coli* PBP 5 (*35*) by a variety of β-lactam antibiotics to 3.3 $\times$ 10^5 M^{-1} s^{-1} for acylation of *Bacillus licheniformis* PBP 1 with benzylpenicillin G (*36*). Moreover, the rate of hydrolysis of [^{14}C]penicillin G bound to PBP 3 was slow ($t_{1/2}$ > 200 min). These results contrast with those of *E. coli* PBP 5, which catalyzes relatively rapid hydrolysis ($t_{1/2}$ ~ 9−10 min) of the acyl-enzyme complex (*32*).

PBP 3 is also an exceptionally active CPase. Characterization of substrate specificity showed that PBP 3 displayed the highest activity (as measured by k_{cat}/K_m) with L-Lys-D-Ala-D-Ala (KAA)-based substrates in which both the α- and ϵ-amino groups of Lys were substituted with bulky substituents, especially the N^{ϵ}-amino group. Significant variation in substrate specificity was observed, with a 20-fold range in k_{cat}/K_m, a 10-fold range in the apparent K_m, and a 2-fold range in the apparent k_{cat} values (Table 2). The k_{cat}/K_m values of up to 1.8 $\times$ 10^5 M^{-1} s^{-1} are very similar to the analogous k_2/K' values for β-lactam binding.

PBPs generally exhibit relatively low catalytic activity compared to other serine hydrolases such as the β-lactamases and serine proteases. Moreover, HMM PBPs show no activity with peptide substrates, although they do undergo acylation with small high-energy ester and thioester substrates (*37*). In contrast, the LMM PBPs, such as PBP 3, catalyze CPase, endopeptidase, and model transpeptidase activities, making them amenable to enzymatic analysis (see Table 5). Even so, the kinetic constants of most of these enzymes are usually very low, with K_m values in the millimolar range and k_{cat}/K_m values between 5 and 100 M^{-1} s^{-1}. For example, PBP 5, a protypical CPase, has a k_{cat}/K_m of 10 M^{-1} s^{-1} and a K_m >20 mM for Ac_2-KAA (*29*). In this context, the k_{cat} values

Table 5: Kinetic Constants of Enzymes Functionally and/or Mechanistically Related to PBP 3

enzyme	source	substrate	k_{cat} (s^{-1})	K_m (mM)	k_{cat}/K_m (M^{-1} s^{-1})	ref
		PBPs/DD-Carboxypeptidases				
DD-peptidase (PBP 3)	*N. gonorrhoeae*	Boc-L-Lys(Cbz)-D-Ala-D-Ala	580	3.3	1.8×10^5	this study
DD-peptidase	*Actinomadura* R39	Ac-L-Lys-D-Ala-D-Ala	18	0.28	6.3×10^4	*55*
DD-peptidase	*Actinomadura* R39	benzoyl-D-Ala-thioglycolate	5.6	0.015	3.7×10^5	*55*
PBP 4a	*B. subtilis*	N^{α}-Ac-L-Lys-D-Ala-D-Ala	−[a]	−	6.7×10^3	*56*
PBP 4a	*B. subtilis*	benzoyl-D-Ala-thioglycolate	23	0.38	6.1×10^4	*56*
PBP 5	*E. coli*	Ac-L-Lys(Ac)-D-Ala-D-Ala	−	−	10	*29*
PBP 5	*E. coli*	Ac-L-Lys(Ac)-D-Ala-D-Lac	20	28	700	*10*
DD-peptidase	*Actinomadura* R39	Ac-L-Lys(Ac)-D-Ala-D-Ala	−	−	5.3×10^4	*57*
DD-peptidase	*Streptomyces* R61	Ac-L-Lys(Ac)-D-Ala-D-Ala	−	−	4.6×10^3	*57*
DD-peptidase	*Streptomyces* R61	glycyl-L-α-amino-ϵ-pimelyl-D-Ala-D-Ala	69	0.0079	8.7×10^6	*38*
DD-peptidase	*Streptomyces* R61	*m*-[[*N*-(phenylacetyl)glycyl]oxy]benzoic acid (acyclic depsipeptide)	1.51	0.76	2×10^3	*58*
DD-peptidase	*Streptomyces* R61	(phenylacetyl)glycylthioglycolic acid (thioester)	2.16	1.45	1.5×10^3	*58*
DD-peptidase	*Streptomyces albus* G	Ac-L-Lys(Ac)-D-Ala-D-Ala	−	−	6×10^3	*57*
t-PBP 3s	*Enterococcus hirae*	benzoyl-D-Ala-D-thio-Gly	6	1.8	3.2×10^3	*37*
PBP 3	*E. coli*	benzoyl-D-Ala-D-thio-Gly	0.25	3	80	*37*
		β-Lactamases				
RTEM β-lactamase	*E. coli*	benzylpenicillin	2000	0.02	1×10^8	*59*
TEM β-lactamase	*E. coli*	benzylpenicillin	782	0.033	2.3×10^7	*60*
class A β-lactamase	*S. albus* G	benzylpenicillin	2800	1	2.8×10^6	*61*
class C β-lactamase	*Enterobacter cloacae* P99	*m*-[[*N*-(phenylacetyl)glycyl]oxy]benzoic acid	125	0.23	5.4×10^5	*58*
class C β-lactamase	*E. cloacae* P99	(phenylacetyl)glycylthioglycolic acid	54	8	6.7×10^3	*58*
		Serine Proteases				
chymotrypsin		AcPhe-*p*-nitrophenyl ester	144	0.0032	4.5×10^7	*62*
chymotrypsin	bovine	succinyl-Ala-Ala-Pro-Phe-*p*-nitroanilide	35	0.093	3.8×10^5	*63*
dipeptidyl peptidase IV	pig kidney	Ala-Pro-*p*-nitroanilide	91	0.014	6.5×10^6	*64*
trypsin	bovine	Cbz-Arg-$SCH_2C_6H_4$	94	0.0053	1.8×10^7	*65*
subtilisin	*B. subtilis*	*o*-aminobenzoyl-DFRLFAF-Tyr(NO_2)	6	0.0002	3×10^7	*66*
elastase	human leukocytes	Me-succinyl-Ala-Ala-Pro-Phe-*p*-nitroanilide	17	0.14	1.2×10^5	*63*
cathepsin G	human leukocytes	succinyl-Ala-Ala-Pro-Phe-*p*-nitroanilide	3.1	2.9	1.1×10^3	*63*

[a] −, not available.

of 260−580 s^{-1} observed for PBP 3 are remarkable, being about 10−100 times higher than those previously reported for other PBPs. Likewise, the k_{cat}/K_m values of 8300−180000 M^{-1} s^{-1} with peptide substrates are also much higher than those observed with most other PBPs. The only PBP with a higher k_{cat}/K_m than PBP 3 is the *Streptomyces* R61 DD-peptidase, with a value of 8.7×10^6 M^{-1} s^{-1} (*38*). Interestingly, the high k_{cat}/K_m value obtained in this study was due to a markedly lower K_m (8 μM) of the novel *Streptomyces*-like substrate, glycyl-L-α-amino-ϵ-pimelyl-D-Ala-D-Ala, used in this study and not to a high k_{cat} (69 s^{-1}).

Kinetic constants for members of two other mechanistically similar enzyme classes, serine proteases and β-lactamases, are shown in Table 5. Proteases have k_{cat}/K_m values up to 10^8 M^{-1} s^{-1} and k_{cat} values up to 150 s^{-1}, but these values are usually obtained only with synthetic ester substrates. The serine β-lactamases, which are evolutionarily related to the PBPs, display k_{cat}/K_m values up to 10^8 M^{-1} s^{-1}, with k_{cat} values up to 3000 s^{-1}. Thus, the k_{cat}/K_m values obtained with PBP 3 are nearing the range observed for β-lactamase-catalyzed hydrolysis of β-lactam substrates. Therefore, despite the low enzymatic activity usually observed for PBP-catalyzed reactions, these enzymes are capable of catalyzing peptidase reactions efficiently.

Depsipeptide substrates for the PBPs often show a large increase in reaction rate over the homologous amide substrates (*39*). Since both the ester (e.g., Ac_2-L-Lys-D-Ala-D-Lac) and amide (e.g., Ac_2-L-Lys-D-Ala-D-Ala) substrates proceed through the same acyl-enzyme intermediate, k_3 will be the same for both substrates (see kinetic scheme in Experimental Procedures). A greater turnover number (k_{cat}) for a depsipeptide substrate is therefore attributed to a higher k_2 and is an indication that k_2 (acylation) is the rate-determining step for hydrolysis of the peptide substrate (*39*, *40*). In contrast, if the peptide and depsipeptide substrates show similar turnover numbers, then k_3 (deacylation) is rate determining, as has been observed previously for PBP 4 from *Staphylococcus aureus* (*39*, *41*). The k_{cat} of PBP 3 for an amide peptide substrate (Ac_2-KAA) was ∼2-fold higher than that against the analogous peptide ester substrate (Ac_2-KA-D-Lac), strongly suggesting that deacylation (k_3) is rate determining ($k_2 \gg k_3$) for PBP 3-catalyzed hydrolysis reactions.

A previous study of *E. coli* PBP 5, which also has a bell-shaped pH profile for CPase activity, gave pK_as of 8.2 and 11.1 (*29*). Thus, compared to PBP 5, the pH profile of PBP 3 (pK_as of 6.8 and 9.8) is shifted significantly toward acidic pHs and is close to the pH profile for class A β-lactamases (pK_as of 5.0−6.2 for the acidic limb, depending on substrate, and 8.5 for the basic limb) (*42*, *43*). These data suggest differences within the active sites of the two CPases such that the active site serine residue in gonococcal PBP 3 is activated at lower pHs. In the absence of a crystal structure, assignment of pK_as to specific active site residues is somewhat speculative. However, given the available biochemical and structural data for β-lactamases and PBPs, one possible candidate for the acidic pK_a of 6.8 is Lys-61 within the SXXK active site motif. In both PBPs and β-lactamases, the equivalent lysine plays a central role in hydrogen bonding in the active site and may act as a general base to activate

the active site serine (*29*, *44*−*47*). Although a pK_a of 6.8 is fairly low for a lysine ϵ-NH_2 group, it is not unprecedented (*29*, *48*). Assignment of the pK_a of the basic limb of the PBP 3 pH profile is more straightforward. On the basis of the highly conserved nature of the lysine in the K(T/S)G active site sequence motif and previous studies on both PBPs and β-lactamases (*29*, *43*), the most probable candidate for the alkaline pK_a is Lys-404, which is the counterpart of Lys-213 in *E. coli* PBP 5 and of Lys-234 in class A β-lactamases.

As demonstrated in this study, PBP 3 is an active CPase and endopeptidase, and it is well established that too much CPase activity causes cell lysis (*32*, *49*, *50*). Indeed, we were unable to express PBP 3 in the periplasm of *E. coli*, even at low, uninduced levels of expression. Given that PBP 3 is the most abundant PBP in gonococcal membranes, as well as an extremely active enzyme, it is unclear how this enzyme functions in gonococcal cell wall biosynthesis, since it might be expected to rapidly hydrolyze pentapeptide cell wall precursors. It seems likely that the CPase activity of PBP 3 is regulated during cell wall synthesis in *N. gonorrhoeae* such that the enzyme is active only at certain times or at specific locations within the cell.

It has been proposed that peptidoglycan is synthesized by a complex of PBPs, lytic transglycosylases, amidases, and scaffolding proteins (*2*, *51*). Moreover, biochemical data in both *E. coli* (*28*) and *Neisseria meningitidis* (*52*) support the existence of such a putative complex. Our results indicate that *N. gonorrhoeae* grows quite well without PBP 3 activity and is only slightly impaired in its growth when missing both PBPs 3 and 4. Thus, assuming that these two enzymes are members of the putative synthetic complex, they clearly are not required for its formation or activity. These data are consistent with a recent study in *E. coli* in which the three main families of murien hydolases, amidases, endopeptidases, and lytic transglycoslases, were examined for their role in cell viability (*53*). The results of that study demonstrated that cells remained viable even after deletion of multiple members of each hydrolase family, although defects in septation were often evident. Thus, it appears as though many of the hydrolytic enzymes, including the endopeptidases, have redundant functions in cell wall biosynthesis.

Even though *N. gonorrhoeae* is viable in the absence of both PBP 3 and PBP 4, SEM revealed that cells lacking both PBPs had marked morphological changes compared to either wild type or the single deletion strains. The double deletion strain was a mixture of normal cells with both large and small cells, suggesting defects in cell division. These data were consistent with our growth rate data, which showed a modest decrease in the doubling time relative to wild type or the single deletion strains. Interestingly, very similar data were observed in *Streptococcus pneumoniae* with PBP 3 mutants (*54*). Pneumococcal PBP 3 is most related to the *E. coli* PBP 5 family of CPases, whereas gonococcal PBP 3 is more related to the *E. coli* PBP 4 family of CPases. Thus, proper balance of transpeptidase (catalyzed by PBPs 1 and 2) versus CPase/endopeptidase (catalyzed by PBPs 3 and 4) activities is required for proper peptidoglycan synthesis and cell division in *N. gonorrhoeae*.

In summary, we describe for the first time that PBP 3 from *N. gonorrhoeae* is an exceptionally active CPase, a DD-endopeptidase, and is inactivated by β-lactam antibiotics with very high k_2/K' constants. The kinetic constants reported here for these activities are unprecedented for a PBP, which generally shows only modest activity in vitro with synthetic substrates. A future goal will be to elucidate the structural basis for this remarkable activity.

ACKNOWLEDGMENT

We thank Christopher Davies at the Medical University of South Carolina for critical reading of the manuscript, Victoria Madden for help with SEM, and Shuqing Zhao for helping to prepare samples for SEM.

REFERENCES

1. Ghuysen, J.-M., and Dive, G. (1994) in *Bacterial Cell Walls* (Ghuysen, J.-M., and Hakenbeck, R., Eds.) pp 103−129, Elsevier Science BV, Amsterdam.
2. Holtje, J. V. (1996) A hypothetical holoenzyme involved in the replication of the murein sacculus of *Escherichia coli*, *Microbiology 142*, 1911−1918.
3. Denome, S. A., Elf, P. K., Henderson, T. A., Nelson, D. E., and Young, K. D. (1999) *Escherichia coli* mutants lacking all possible combinations of eight penicillin binding proteins: viability, characteristics, and implications for peptidoglycan synthesis, *J. Bacteriol. 181*, 3981−3993.
4. Barbour, A. G. (1981) Properties of penicillin-binding proteins in *Neisseria gonorrhoeae*, *Antimicrob. Agents Chemother. 19*, 316−322.
5. Ropp, P. A., and Nicholas, R. A. (1997) Cloning and characterization of the *ponA* gene encoding penicillin-binding protein 1 from *Neisseria gonorrhoeae* and *Neisseria meningitidis*, *J. Bacteriol. 179*, 2783−2787.
6. Spratt, B. G. (1988) Hybrid penicillin-binding proteins in penicillin-resistant strains of *Neisseria gonorrhoeae*, *Nature 332*, 173−176.
7. Ropp, P. A., Hu, M., Olesky, M., and Nicholas, R. A. (2002) Mutations in *ponA*, the gene encoding penicillin-binding protein 1, and a novel locus, *penC*, are required for high-level chromosomally mediated penicillin resistance in *Neisseria gonorrhoeae*, *Antimicrob. Agents Chemother. 46*, 769−777.
8. Dougherty, T. J., Koller, A. E., and Tomasz, A. (1980) Penicillin-binding proteins of penicillin-susceptible and intrinsically resistant *Neisseria gonorrhoeae*, *Antimicrob. Agents Chemother. 18*, 730−737.
9. Gutheil, W. G., Stefanova, M. E., and Nicholas, R. A. (2000) Fluorescent coupled enzyme assays for D-alanine: application to penicillin-binding protein and vancomycin activity assays, *Anal. Biochem 287*, 196−202.
10. Gutheil, W. G. (1998) A sensitive equilibrium-based assay for D-lactate using D-lactate dehydrogenase: application to penicillin-binding protein/DD-carboxypeptidase activity assays, *Anal. Biochem 259*, 62−67.
11. Pechenov, A., Stefanova, M. E., Nicholas, R. A., Peddi, S., and Gutheil, W. G. (2003) Potential transition state analogue inhibitors for the penicillin-binding proteins, *Biochemistry 42*, 579−588.
12. Sarubbi, F. A. J., Blackman, E., and Sparling, P. F. (1974) Genetic mapping of linked antibiotic resistance loci in *Neisseria gonorrhoeae*, *J. Bacteriol. 120*, 1284−1292.
13. Kellogg, D. S., Peacock, W. L., Deacon, W. E., Browh, L., and Perkle, C. I. (1963) *Neisseria gonorrhoeae*. I. Virulence genetically linked to colonial variation, *J. Bacteriol. 85*, 1274−1279.
14. Prentki, P., and Krisch, H. M. (1984) In vitro insertional mutagenesis with a selectable DNA fragment, *Gene 29*, 303−313.
15. Delahay, R. M., Robertson, B. D., Balthazar, J. T., Shafer, W. M., and Ison, C. A. (1997) Involvement of the gonococcal MtrE protein in the resistance of *Neisseria gonorrhoeae* to toxic hydrophobic agents, *Microbiology 143*, 2127−2133.
16. Blaszczak, L. C., Halligan, N. G., and Seitz, D. E. (1989) Radioiododestannylation. Convenient synthesis of a stable penicillin derivative for rapid penicillin binding protein (PBP) assay, *J. Labelled Compd. Radiopharm. 27*, 401−406.
17. Frere, J. M., Nguyen-Disteche, M., Coyette, J., and Joris, B. (1992) in *The Chemistry of β-Lactams*, pp 148−196, Chapman & Hall, Glasgow.
18. Perkins, H. R., Nieto, M., Frere, J. M., Leyh-Bouille, M., and Ghuysen, J. M. (1973) *Streptomyces* DD-carboxypeptidases as

transpeptidases. The specificity for amino compounds acting as carboxyl acceptors, *Biochem. J. 131*, 707−718.
19. Tamura, T., Imae, Y., and Strominger, J. L. (1976) Purification to homogeneity and properties of two D-alanine carboxypeptidases I from *Escherichia coli*, *J. Biol. Chem. 251*, 414−423.
20. Frère, J. M., Leyh-Bouille, M., Ghuysen, J. M., Nieto, M., and Perkins, H. R. (1976) Exocellular DD-carboxypeptidases-transpeptidases from *Streptomyces*, *Methods Enzymol. 45*, 610−636.
21. Glauner, B. (1988) Separation and quantification of muropeptides with high-performance liquid chromatography, *Anal. Biochem. 172*, 451−464.
22. Glauner, B., Holtje, J. V., and Schwarz, U. (1988) The composition of the murein of *Escherichia coli*, *J. Biol. Chem. 263*, 10088−10095.
23. Nielsen, H., Engelbrecht, J., Brunak, S., and von Heijne, G. (1997) Identification of prokaryotic and eukaryotic signal peptides and prediction of their cleavage sites, *Protein Eng. 10*, 1−6.
24. Nakai, K., and Kanehisa, M. (1991) Expert system for predicting protein localization sites in gram-negative bacteria, *Proteins 11*, 95−110.
25. Mottl, H., and Keck, W. (1991) Purification of penicillin-binding protein 4 of *Escherichia coli* as a soluble protein by dye-affinity chromatography, *Eur. J. Biochem. 200*, 767−773.
26. Spratt, B. G. (1975) Distinct penicillin-binding proteins involved in the division, elongation, and shape of *Escherichia coli*, *Proc. Natl. Acad. Sci. U.S.A. 72*, 2999−3003.
27. Zijderveld, C. A., Aarsman, M. E., den Blaauwen, T., and Nanninga, N. (1991) Penicillin-binding protein 1B of *Escherichia coli* exists in dimeric forms, *J. Bacteriol. 173*, 5740−5746.
28. Vollmer, W., von Rechenberg, M., and Holtje, J. V. (1999) Demonstration of molecular interactions between the murein polymerase PBP1B, the lytic transglycosylase MltA, and the scaffolding protein MipA of *Escherichia coli*, *J. Biol. Chem. 274*, 6726−6734.
29. Stefanova, M. E., Davies, C., Nicholas, R. A., and Gutheil, W. G. (2002) pH, inhibitor, and substrate specificity studies on *Escherichia coli* penicillin-binding protein 5, *Biochim. Biophys. Acta 1597*, 292−300.
30. Matsuhashi, M., Maruyama, I. N., Takagaki, Y., Tamaki, S., Nishimura, Y., and Hirota, Y. (1978) Isolation of a mutant of *Escherichia coli* lacking penicillin-sensitive D-alanine carboxypeptidase 1A, *Proc. Natl. Acad. Sci. U.S.A. 75*, 2631−2635.
31. Schultz, D. E., Spratt, B. G., and Nicholas, R. A. (1991) Expression and purification of a soluble form of penicillin-binding protein 2 from both penicillin-susceptible and penicillin-resistant *Neisseria gonorrhoeae*, *Protein Expression Purif. 2*, 339−349.
32. Nicholas, R. A., and Strominger, J. L. (1988) Site-directed mutants of a soluble form of penicillin-binding protein 5 from *Escherichia coli* and their catalytic properties, *J. Biol. Chem. 263*, 2034−2040.
33. Palomeque-Messia, P., Quittre, V., Leyh-Bouille, M., Nguyen-Disteche, M., Gershater, C. J., Dacey, I. K., Dusart, J., Van Beeumen, J., and Ghuysen, J. M. (1992) Secretion by overexpression and purification of the water-soluble *Streptomyces* K15 DD-transpeptidase/penicillin-binding protein, *Biochem. J. 288*, 87−91.
34. Fonze, E., Vermeire, M., Nguyen-Disteche, M., Brasseur, R., and Charlier, P. (1999) The crystal structure of a penicilloyl-serine transferase of intermediate penicillin sensitivity. The DD-transpeptidase of *Streptomyces* K15, *J. Biol. Chem. 274*, 21853−21860.
35. Beadle, B. M., Nicholas, R. A., and Shoichet, B. K. (2001) Interaction energies between β-lactam antibiotics and *E. coli* penicillin-binding protein 5 by reversible thermal denaturation, *Protein Sci. 10*, 1254−1259.
36. Lepage, S., Galleni, M., Lakaye, B., Joris, B., Thamm, I., and Frere, J. M. (1995) Kinetic properties of the *Bacillus licheniformis* penicillin-binding proteins, *Biochem. J. 309*, 49−53.
37. Adam, M., Damblon, C., Jamin, M., Zorzi, W., Dusart, V., Galleni, M., el Kharroubi, A., Piras, G., Spratt, B. G., Keck, W., et al. (1991) Acyltransferase activities of the high-molecular-mass essential penicillin-binding proteins, *Biochem. J. 279*, 601−604.
38. Anderson, J. W., and Pratt, R. F. (2000) Dipeptide binding to the extended active site of the *Streptomyces* R61 D-alanyl-D-alanine-peptidase: the path to a specific substrate, *Biochemistry 39*, 12200−12209.
39. Rasmussen, J. R., and Strominger, J. L. (1978) Utilization of a depsipeptide substrate for trapping acyl-enzyme intermediates of penicillin-sensitive D-alanine carboxypeptidases, *Proc. Natl. Acad. Sci. U.S.A. 75*, 84−88.
40. Xu, Y., Soto, G., Hirsch, K. R., and Pratt, R. F. (1996) Kinetics and mechanism of the hydrolysis of depsipeptides catalyzed by the β−lactamase of *Enterobacter cloacae* P99, *Biochemistry 35*, 3595−3603.
41. Kozarich, J. W., and Strominger, J. L. (1978) A membrane enzyme from *Staphylococcus aureus* which catalyzes transpeptidase, carboxypeptidase, and penicillinase activities, *J. Biol. Chem. 253*, 1272−1278.
42. Lietz, E. J., Truher, H., Kahn, D., Hokenson, M. J., and Fink, A. L. (2000) Lysine-73 is involved in the acylation and deacylation of β-lactamase, *Biochemistry 39*, 4971−4981.
43. Ellerby, L. M., Escobar, W. A., Fink, A. L., Mitchinson, C., and Wells, J. A. (1990) The role of lysine-234 in β-lactamase catalysis probed by site-directed mutagenesis, *Biochemistry 29*, 5797−5806.
44. Zawadzke, L. E., Chen, C. C., Banerjee, S., Li, Z., Wasch, S., Kapadia, G., Moult, J., and Herzberg, O. (1996) Elimination of the hydrolytic water molecule in a class A β-lactamase mutant: crystal structure and kinetics, *Biochemistry 35*, 16475−16482.
45. Strynadka, N. C., Adachi, H., Jensen, S. E., Johns, K., Sielecki, A., Betzel, C., Sutoh, K., and James, M. N. (1992) Molecular structure of the acyl-enzyme intermediate in β-lactam hydrolysis at 1.7 Å resolution, *Nature 359*, 700−705.
46. Maveyraud, L., Pratt, R. F., and Samama, J. P. (1998) Crystal structure of an acylation transition-state analog of the TEM-1 β-lactamase. Mechanistic implications for class A β-lactamases, *Biochemistry 37*, 2622−2628.
47. Davies, C., White, S. W., and Nicholas, R. A. (2001) Crystal structure of a deacylation-defective mutant of penicillin-binding protein 5 at 2.3-Å resolution, *J. Biol. Chem. 276*, 616−623.
48. Fersht, A. R. (1985) *Enzyme Structure and Mechanism*, 2nd ed., W. H. Freeman and Co., New York.
49. Markiewicz, Z., Broome-Smith, J. K., Schwarz, U., and Spratt, B. G. (1982) Spherical *E. coli* due to elevated levels of D-alanine carboxypeptidase, *Nature 297*, 702−704.
50. Nelson, D. E., Ghosh, A. S., Paulson, A. L., and Young, K. D. (2002) Contribution of membrane-binding and enzymatic domains of penicillin binding protein 5 to maintenance of uniform cellular morphology of *Escherichia coli*, *J. Bacteriol. 184*, 3630−3639.
51. von Rechenberg, M., Ursinus, A., and Holtje, J. V. (1996) Affinity chromatography as a means to study multienzyme complexes involved in murein synthesis, *Microb. Drug Resist. 2*, 155−157.
52. Jennings, G. T., Savino, S., Marchetti, E., Arico, B., Kast, T., Baldi, L., Ursinus, A., Holtje, J. V., Nicholas, R. A., Rappuoli, R., and Grandi, G. (2002) GNA33 from *Neisseria meningitidis* serogroup B encodes a membrane-bound lytic transglycosylase (MltA), *Eur. J. Biochem. 269*, 3722−3731.
53. Heidrich, C., Ursinus, A., Berger, J., Schwarz, H., and Holtje, J. V. (2002) Effects of multiple deletions of murein hydrolases on viability, septum cleavage, and sensitivity to large toxic molecules in *Escherichia coli*, *J. Bacteriol. 184*, 6093−6099.
54. Schuster, C., Dobrinski, B., and Hakenbeck, R. (1990) Unusual septum formation in *Streptococcus pneumoniae* mutants with an alteration in the D,D-carboxypeptidase penicillin-binding protein 3, *J. Bacteriol. 172*, 6499−6505.
55. Zhao, G. H., Duez, C., Lepage, S., Forceille, C., Rhazi, N., Klein, D., Ghuysen, J. M., and Frere, J. M. (1997) Site-directed mutagenesis of the *Actinomadura* R39 DD-peptidase, *Biochem. J. 327*, 377−381.
56. Duez, C., Vanhove, M., Gallet, X., Bouillenne, F., Docquier, J., Brans, A., and Frere, J. (2001) Purification and characterization of PBP4a, a new low-molecular-weight penicillin-binding protein from *Bacillus subtilis*, *J. Bacteriol. 183*, 1595−1599.
57. Adam, M., Damblon, C., Plaitin, B., Christiaens, L., and Frere, J. M. (1990) Chromogenic depsipeptide substrates for β-lactamases and penicillin-sensitive DD-peptidases, *Biochem. J. 270*, 525−529.
58. Adediran, S. A., and Pratt, R. F. (1999) B-secondary and solvent deuterium kinetic isotope effects on catalysis by the Streptomyces R61 DD-peptidase: comparisons with a structurally similar class C β-lactamase, *Biochemistry 38*, 1469−1477.
59. Fisher, J., Belasco, J. G., Khosla, S., and Knowles, J. R. (1980) β-Lactamase proceeds via an acyl-enzyme intermediate. Interaction of the *Escherichia coli* RTEM enzyme with cefoxitin, *Biochemistry 19*, 2895−2901.
60. Osuna, J., Viadiu, H., Fink, A. L., and Soberon, X. (1995) Substitution of Asp for Asn at position 132 in the active site of TEM β-lactamase. Activity toward different substrates and effects of neighboring residues, *J. Biol. Chem. 270*, 775−780.

61. Matagne, A., Misselyn-Bauduin, A. M., Joris, B., Erpicum, T., Granier, B., and Frere, J. M. (1990) The diversity of the catalytic properties of class A β-lactamases, *Biochem. J. 265*, 131−146.
62. Fastrez, J., and Fersht, A. R. (1973) Demonstration of the acyl-enzyme mechanism for the hydrolysis of peptides and anilides by chymotrypsin, *Biochemistry 12*, 2025−2034.
63. Nakajima, K., Powers, J. C., Ashe, B. M., and Zimmerman, M. (1979) Mapping the extended substrate binding site of cathepsin G and human leukocyte elastase. Studies with peptide substrates related to the alpha 1-protease inhibitor reactive site, *J. Biol. Chem. 254*, 4027−4032.
64. Gutheil, W. G., and Bachovchin, W. W. (1993) Separation of L-Pro-DL-boroPro into its component diastereomers and kinetic analysis of their inhibition of dipeptidyl peptidase IV. A new method for the analysis of slow, tight-binding inhibition, *Biochemistry 32*, 8723−8731.
65. Cook, R. R., McRae, B. J., and Powers, J. C. (1984) Kinetics of hydrolysis of peptide thioester derivatives of arginine by human and bovine thrombins, *Arch. Biochem. Biophys. 234*, 82−88.
66. Grøn, H., and Breddam, K. (1992) Interdependency of the binding subsites in subtilisin, *Biochemistry 31*, 8967−8971.

BI0350607